TV or not TV? That is the Question

Christian Riess, Martin Berger, Haibo Wu, Michael Manhart, Rebecca Fahrig and Andreas Maier

***Abstract*—Iterative reconstruction methods with regularization become more and more popular. In the literature, amazing results are reported that are able to reconstruct images from very few views and from trajectories that do not acquire complete data sets such as would be required for analytical reconstruction methods.**

A large disadvantage of iterative methods is their high computational demand. Bruder et al. have shown that if the reconstruction is accurate enough, the regularization can be performed in the reconstructed image only which allows for much faster application of the regularization term.

In this paper, we present a heuristic compensation weight that corrects for the loss of mass in a filtered back-projection type reconstruction given a limited angle problem. Although the reconstruction contains artifacts, we show that the application of a bilateral filter in the reconstruction domain is able to recover almost the same signal as a TV-regularized iterative reconstruction. The reconstruction error is reduced from 0.130 to 0.057 which is the same as for the iterative case.

I. Introduction

Iterative reconstruction methods that use some kind of regularization are becoming more and more popular. Using certain assumptions, such as that the object of interest is piece-wise constant, allows violation of the Nyquist-Shannon sampling theorem [1], [2]. Reconstruction time, however, is often dramatically increased. Iterative regularized reconstructions are only feasible, if they are implemented on special hardware such as graphics cards. Still, the reconstruction time is an order of magnitude higher than the reconstruction time in a traditional filtered back-projection algorithm.

Recently, novel approaches have been presented providing typical benefits of iterative algorithms, but are based on a filtered back-projection (FBP) type algorithm. Hence, they do not have to project forward and backward repeatedly in their iterations. Bruder et al. have shown that there exists an image-based non-linear filter that is equivalent to a full iterative reconstruction with regularization [3]. However, the method can only be applied if the initial reconstruction is sufficiently accurate. Zeng presented an FBP-type algorithm, which has similar characteristics to those of an iterative MAP (maximum *a posteriori*) algorithm [4].

In general, analytic reconstruction methods face a challenge if they have to reconstruct data from an incomplete trajectory [5], [6]. A fan beam trajectory is complete, if $180^\circ + 2\delta_{\max}$ are acquired, where $\delta_{\max}$ is the half fan angle. This is often referred to as a short scan in the literature. Redundant rays can be weighted which provides a correct reconstruction [7]. Extensions to this weighting to incorporate larger areas of redundancy [8] and to optimize the signal-to-noise-ratio [9] exist. If less than a short scan is acquired, analytic reconstruction is still possible, but the field-of-view (FOV) that allows correct reconstruction is reduced [10]. In contrast, iterative methods using regularization based on total variation (TV) minimization allow the correct reconstruction of the complete FOV, if the object of interest is piece-wise constant [1].

In this paper, we investigate this mismatch. We further propose to use a compensation weight that is a heuristic extension of the commonly used redundancy weights to improve the analytical reconstruction. In order to obtain the final reconstruction, we then apply an image-based regularization using a bilateral filter that enforces piece-wise constancy. Results indicate that this analytical reconstruction delivers reconstructions that are very close to the iterative reconstruction method. Computation time, however, is an order of magnitude lower compared to the iterative procedure.

II. Methods

In the following section, we will shortly describe the used reconstruction methods, beginning with the iterative TV-regularized reconstruction. Next, the analytic reconstruction methods and the different redundancy weights are detailed. At the end of this section, we describe the error metrics that are used in the results section.

A. Iterative Reconstruction

As a reference reconstruction system, we used an iterative reconstruction with an augmented objective function

$$\min_{\mathbf{x}} \|\mathbf{x}\|_{\mathrm{TV}} \quad \text{subject to} \quad \|\mathbf{A}\mathbf{x} - \mathbf{b}\|_2^2$$

where $\mathbf{x}$ denotes the reconstruction volume, $\mathbf{A}$ the system matrix that projects $\mathbf{x}$ on the detector where the line integrals $\mathbf{b}$ are measured. Details on the implementation are given in [11].

B. Analytic Reconstruction

In the following, we describe the analytical reconstruction algorithm using a 2D formulation. Note that any of the presented concepts can easily be extended to a 3D reconstruction using a Feldkamp-like approximation. The image $f(x, y)$ is reconstructed using a filtered back-projection

$$f(x,y) = \int \frac{1}{U^2} \int \frac{D}{\sqrt{D^2 + s^2}} w(s,\lambda) g(s,\lambda) h_R(s' - s) \mathrm{d}s \mathrm{d}\lambda$$

where D is the distance from the source to the center of rotation, U the depth of the reconstruction point (x, y) and

Christian Riess and Rebecca Fahrig are with the Department of Radiology, Stanford University, Stanford, CA, USA. Martin Berger, Haibo Wu, Michael Manhart and Andreas Maier are with the Pattern Recognition Lab, Department of Computer Science, Friedrich-Alexander-Universität Erlangen-Nürnberg. The authors gratefully acknowledge funding of the Erlangen Graduate School in Advanced Optical Technologies (SAOT) by the German Research Foundation (DFG) in the framework of the German excellence initiative and the Erlangen Graduate School Heterogeneous Imaging Systems.

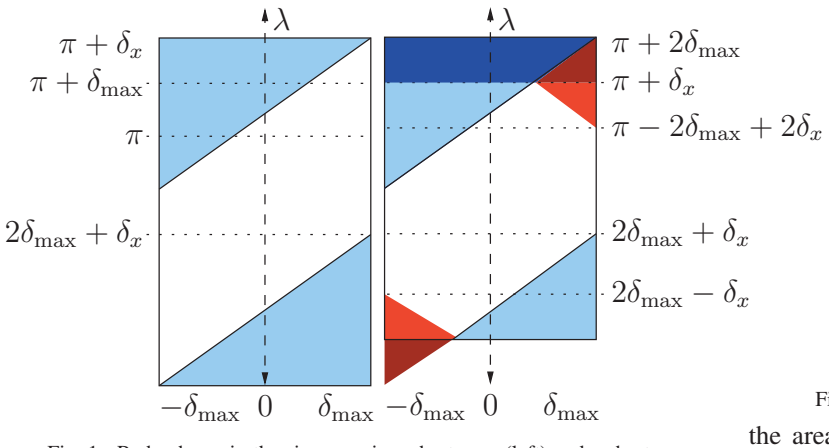

Fig. 1. Redundancy in the sinogram in a short scan (left) and a shorter scan: While the short scan addresses only double rays in the light blue areas, the shorter scan is also missing angles for the complete VOI in the dark red areas.

s' its projection onto the detector $g(s,\lambda)$ at gantry rotation λ. s denotes the detector element and $w(s,\lambda)$ a redundancy weight that deals with inconsistent rays. For convenience, we have virtually placed the detector into the center of rotation.

1) Redundancy Weights: To eliminate artifacts in the reconstruction that are caused by rays which were acquired twice, we use a redundancy weight as described in [8]. Let

$$\eta(\lambda,\delta) = \sin^2\left(\frac{\pi}{2}\frac{\pi+\delta_x-\lambda}{\delta_x-2\delta}\right) \quad \text{and} \tag{1}$$

$$\zeta(\lambda,\delta) = \sin^2\left(\frac{\pi}{2}\frac{\lambda}{\delta_x+2\delta}\right) \tag{2}$$

denote the redundancy weights at the beginning and the end of the scan, respectively. The weights $w_r(s,\lambda)$ are then computed as

$$w_r(s,\lambda) = \begin{cases} \eta(\lambda,\delta) & \text{if} \quad \pi+2\delta \le \lambda \le \pi+\delta_x \\ \zeta(\lambda,\delta) & \text{if} \quad 0 \le \lambda \le 2\delta+\delta_x \\ 1 & \text{otherwise} \end{cases}$$

In this formulation, δ denotes the angle associated with detector element s and δ_x is the scan range in which the redundancy occurs. If $\delta_x = 2\delta_{\max}$ Parker's original formulation is obtained [7]. Note that this formulation is also correct for $\delta_x < 2\delta_{\max}$. The only problem that occurs is that some of the projections ($\lambda = 0$ and $\lambda = \pi+\delta_x$) would get assigned a weight that is 1 for the non-redundant part and 0 for the redundant part. The resulting step function would cause artifacts in the subsequent reconstruction. In order to omit artifacts, we applied a low-pass filter on the weights in these projections.

2) Compensation Weights: Figure 1 shows the difference between a short scan and a scan configuration with $\delta_x < 2\delta_{\max}$. While the short scan only has to solve the redundancy in the triangles described by $\pi+2\delta \le \lambda \le \pi+\delta_x$ and $0 \le \lambda \le 2\delta+\delta_x$ that are shown in light blue in the figure, the shorter scan is missing information in the triangle $\pi+\delta_x \le \lambda \le \pi+2\delta$ that is shown in dark red. The missing data will cause artifacts in the resulting reconstruction. Most of the artifacts are caused by the missing mass during the back-projection. The signal reduction is proportional to the amount of missing angles. The rays in the triangles $\pi+2\delta_x-2\delta \le \lambda \le \pi+\delta_x$ and $0 \le \lambda \le -\delta_x-2\delta$ that are shown in light red pass through

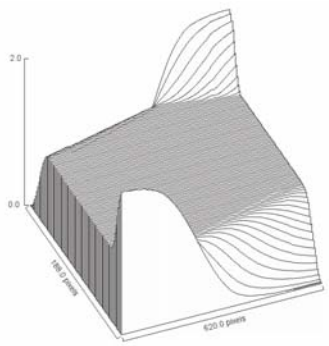

Fig. 2. Surface plot of an instance of compensation weights.

the area where the mass in the reconstruction is missing. In order to create a reconstruction with equal mass distribution, we now increase the weight of these rays with the following compensation weight $w_c(s,\lambda)$:

$$w_c(s,\lambda) = \begin{cases} \eta(\lambda,\delta) & \text{if} \quad \pi+2\delta \le \lambda \le \pi+\delta_x \\ 2-\eta(\lambda,\delta) & \text{if} \quad \pi+2\delta_x-2\delta \le \lambda \le \pi+\delta_x \\ \zeta(\lambda,\delta) & \text{if} \quad 0 \le \lambda \le 2\delta+\delta_x \\ 2-\zeta(\lambda,\delta) & \text{if} \quad 0 \le \lambda \le -\delta_x-2\delta \\ 1 & \text{otherwise} \end{cases}$$

Note that for the projections at $\lambda = 0$ and $\lambda = \pi+\delta_x$ the weight takes the form of a step function as in the case of the redundancy weights. We alleviated the problem by the same low-pass filter as in the case of the redundancy weights. Figure 2 demonstrates the shape of the compensation weights.

3) Bilateral Filtering: The bilateral filter, originally proposed by Tomasi and Manduchi [12], is a smoothing operator that protects sharp edges. The idea is that the spatial support for a Gaussian operator is weighted. More specifically, let $f(x,y)$ and $f^*(x,y)$ denote an intensity in the image at position (x,y) and its bilaterally filtered output, respectively. Here, $f^*(x,y)$ is computed by

$$f^*(x,y) = \sum_{(x',y')\in\mathcal{N}} g(\|(x',y')^{\mathrm{T}} - (x,y)^{\mathrm{T}}\|_2, \sigma_{g,1}) \cdot g(|f(x,y) - f(x',y')|, \sigma_{g,2}) \tag{3}$$

where $g(\mu,\sigma)$ denotes the Gaussian function with mean μ and standard deviation σ, and $\mathcal{N}$ denotes the set of all pixels within a spatially close distance to (x,y).

C. Metrics

For quantitative comparison of the results, we compute three distance metrics, namely the mean square error (MSE), the relative root mean square error (rRMSE) and the structural similarity index (SSID).

The mean square error denotes the pixelwise squared difference between the reconstructed volume and our ground truth, the Shepp-Logan phantom. The relative root mean square error (rRMSE) is similar to the MSE, but normalized with respect to the variations in the image. Thus, it is defined as

$$\epsilon_{\mathrm{rRMSE}} = \frac{\|\mathbf{x}-\tilde{\mathbf{x}}\|_2}{\|\tilde{\mathbf{x}}\|} \quad , \tag{4}$$

where $\mathbf{x}$ and $\tilde{\mathbf{x}}$ denote the reconstructed intensities and the ground truth phantom, respectively.

The structural similarity index is a widespread metric that is based on the standard deviation of the reconstructed signal. It is defined as

$$\frac{4 \cdot \mathrm{cov}(\mathbf{x}, \tilde{\mathbf{x}}) \cdot \mu\tilde{\mu}}{(\mu^2 + \tilde{\mu}^2) \cdot (\sigma^2 + \tilde{\sigma}^2)} \quad , \tag{5}$$

where σ and $\tilde{\sigma}$ denote the standard deviations of the reconstructed image $\mathbf{x}$ and the ground truth $\tilde{\mathbf{x}}$, respectively. $\mathrm{cov}(\mathbf{x}, \tilde{\mathbf{x}})$ denotes the covariance between the images. μ and $\tilde{\mu}$ are the mean values of $\mathbf{x}$ and $\tilde{\mathbf{x}}$, respectively.

III. Results

In our experiments, we demonstrate that we achieve a similar image quality using compensation weights and bilateral filtering compared to a state-of-the-art TV-regularized iterative reconstruction [11].

A. Experimental Setup

We evaluated our approach on a simulated 3D Shepp-Logan phantom [13]. For the projection, we used a detector with 640 detector elements of size 0.5 mm and we sampled the phantom at 180 angles with an angular increment of 1. Source to Detector distance was chosen to be 500 mm. The detector was virtually placed into the center of rotation. The phantom was scaled to fill the FOV without truncation As a result of this configuration, the redundancy weighted reconstruction (see next Section) suffers from an undersampled region in the upper part of the image.

B. Qualitative Assessment

Figure 3 shows the qualitative results for the proposed method. On the left, the Shepp-Logan phantom and the result for total variation regularization are shown. In the middle column, the reconstruction results for the classical redundancy weights are shown, with and without bilateral filtering. The right column shows the reconstruction result for the proposed compensation weights.

As expected, Parker weights are not able to reconstruct the area with missing angles correctly. This leads to the dark area in the upper part of the phantom. The TV-regularized reconstruction yields an excellent result. In particular, the sparsity constraint of the algorithm almost perfectly restores the phantom. The reconstruction using compensation weights results in an image with a large number of high frequency streak artifacts that result from the remaining missing information. However, bilateral filtering almost completely removes these artifacts, yielding a result that is comparable to the TV reconstruction result. The same observations can be obtained by looking at the line profiles shown in Figure 4.

C. Quantitive Assessment

For quantitative evaluation, we selected a region of interest (ROI) in the upper part of the phantom, i. e. where the undersampling occurs. Figure 3a shows the region where the ROI was selected.

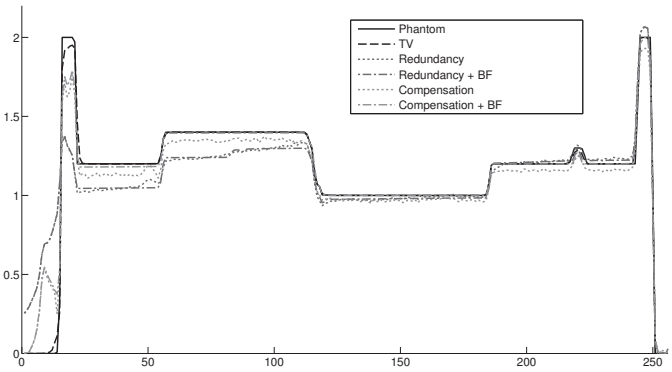

Fig. 4. Intensity profile along a vertical line through the phantom.

	rRMSE	MSE	SSIM
Redundancy	0.1301	0.0286	0.9528
Redundancy BF	0.1271	0.0273	0.9594
Compensation	0.0673	0.0076	0.9594
Compensation BF	0.0569	0.0055	0.9673
TV	0.0566	0.0054	0.9777

TABLE I
Quantitative measurements.

Table I shows the results of the quantitative measurements. The result of the qualitative assessment is confirmed by all reported measures. The quality of the TV-regularized reconstruction is the best. The reconstruction with compensation weights is very close to this result.

IV. Discussion

Our observations confirm the findings by Bruder et al. [3]. We are able to enforce the regularization by applying a bilateral filter in the reconstruction domain only. This enables us to recover a reconstruction that is comparable to a TV-regularized reconstruction. As commented by Bruder et al. the reconstruction must yield an image quality that is sufficient to enforce the regularization in the reconstruction domain. This is usually not the case in limited angle reconstructions as the missing data leads to a deterministic decrease of reconstruction values in the area with missing angle. We compensate for this using a heuristic weighting procedure that increases weights according to the amount of missing data. Thus we are able to create a reconstruction that is improved but still suffers from streak artifacts. The magnitude of these artifacts, however, is an order of magnitude lower than the artifact resulting from the missing angle. Subsequent use of a bilateral filter is able to recover the original signal.

In the present study, we used a simple phantom that is very popular when exploring reconstructions using TV-regularization. We expect similar results when using other piece-wise constant phantoms [14]. Note that the results presented here required the 8-fold application of the bilateral filter. Still the processing time was an order of magnitude lower than the processing time of the iterative reconstruction with 1000 iterations.

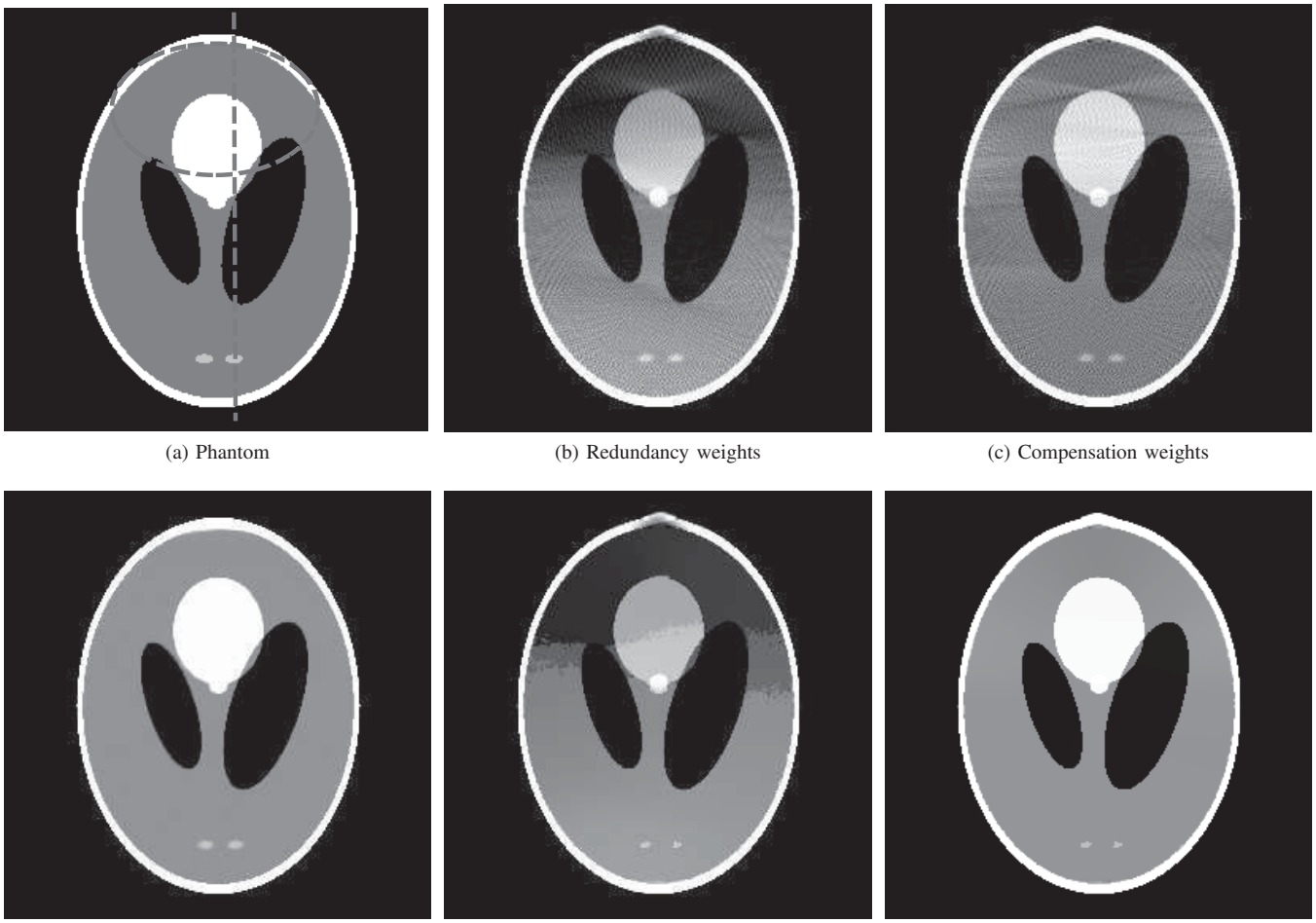

(a) Phantom (b) Redundancy weights (c) Compensation weights

(d) TV-regularized (e) Redundancy weights+BF (f) Compensation weights+BF

Fig. 3. Qualitative comparison of the reconstructed slices: The compensation weights in combination with a bilateral filter (BF) visually appears almost identical to a TV-regularized reconstruction. The window for the visualization was chosen as [1.0, 1.4].

In real data, results may be quite different. However, we still expect that our method is suited to initialize an iterative reconstruction and will therewith decrease the number of required iterations.

V. Conclusion

We have shown a compensation method that allows reconstruction of images that are comparable to the reconstructions created with a TV-regularized iterative reconstruction. The result of the proposed method can be computed within seconds, while the iterative procedure has a computation time that is an order of magnitude higher.

References

[1] E. Sidky, C. Kao, and X. Pan, "Accurate image reconstruction from few-views and limited-angle data in divergent-beam ct," *Journal of X-ray Science and Technology*, vol. 14, no. 2, pp. 119–139, 2006.

[2] X. Pan, E. Sidky, and M. Vannier, "Why do commercial CT scanners still employ traditional, filtered back-projection for image reconstruction?" *Inverse problems*, vol. 25, no. 12, pp. 1–50, 2009. [Online]. Available: http://iopscience.iop.org/0266-5611/25/12/123009

[3] H. Bruder, R. Raupach, J. Sunnegardh, M. Sedlmair, K. Stierstorfer, and T. Flohr, "Adaptive iterative reconstruction," in *SPIE Medical Imaging*, vol. 7961, 2011, pp. 79 610J–79 610J–12. [Online]. Available: http://dx.doi.org/10.1117/12.877953

[4] G. L. Zeng, "View-based noise modeling in the filtered backprojection MAP algorithm," in *Proc. of the 2nd CT Meeting*, 2012, pp. 103–106.

[5] T. M. Buzug, *Computed Tomography*. Berlin, Germany: Springer, 2008.

[6] G. L. Zeng, *Medical Image Reconstruction: A Conceptual Tutorial*. Berlin, Germany: Springer, 2009.

[7] D. L. Parker, "Optimal short scan convolution reconstruction for fan-beam CT," *Medical Physics*, vol. 9, no. 2, pp. 254–257, 1982.

[8] M. D. Silver, "A method for including redundant data in computed tomography," *Medical Physics*, vol. 27, no. 4, pp. 773–774, 2000.

[9] S. Wesarg, M. Ebert, and T. Bortfeld, "Parker weights revisited," *Medical Physics*, vol. 29, no. 3, pp. 372–378, 2002.

[10] F. Noo, M. Defrise, R. Clackdoyle, and H. Kudo, "Image reconstruction from fan-beam projections on less than a short scan," *Physics in Medicine and Biology*, vol. 47, no. 14, pp. 2525–2546, 2002.

[11] H. Wu, C. Rohkohl, and J. Hornegger, "Total Variation Regularization Method for 3-D Rotational Coronary Angiography," in *Bildverarbeitung für die Medizin 2011*, Lübeck, Germany, 2011, pp. 434–438.

[12] C. Tomasi and R. Manduchi, "Bilateral filtering for gray and color images," in *Sixth International Conference on Computer Vision*. Washington, DC, USA: IEEE Computer Society, 1998, pp. 839–846.

[13] L. A. Shepp and B. F. Logan, "The Fourier reconstruction of a head section-LA Shepp," *IEEE Transactions on Nuclear Science*, vol. NS-21, pp. 21–43, 1974.

[14] A. Maier, H. G. Hofmann, C. Schwemmer, J. Hornegger, A. Keil, and R. Fahrig, "Fast simulation of x-ray projections of spline-based surfaces using an append buffer." *Physics in medicine and biology*, vol. 57, no. 19, pp. 6193–210, Oct. 2012. [Online]. Available: http://stacks.iop.org/0031-9155/57/i=19/a=6193